A Closed Loop Transmission Power Control System using a Nonlinear Approximation of Power-Time Curve

Andre M. Mayers, *Member IEEE,* Patrick Benavidez, *Member IEEE,* D. Akopian, *Member IEEE*, GVS Raju, *Fellow IEEE*, David Akopian*, Member IEEE,* and Mo Jamshidi, *Fellow IEEE*

***Abstract*— In wireless communication networks, it is desirable to achieve energy efficiency while maintaining quality of service (QoS). Overall energy efficiency can be achieved by minimizing the power output for each communication device. This paper presents a novel energy saving adaptive transmit power control (TPC) algorithm based on bit error rate (BER) feedback (BER-TPC) that outperforms conventional approaches based on signal-to-interference-plus-noise ratio (SINR) feedback (SINR-TPC). It is a distributed algorithm deployed in both transmitting and receiving devices that can be applied for various wireless network topologies and protocols. The paper addresses the power efficiency of adaptive TPC in terms of reduced total transmit power of the network by smoothing transmit power transients during adaptive iterations. It is achieved using a distributed closed loop power control system that applies heuristically estimated dual-rate power adjustments during adaptive iterations. Because the proposed system uses a mathematical formula for power adjustment, operational bounds for stability can be provided using simple analysis. It is demonstrated that the proposed system provides adequate tradeoff between performance and complexity in terms of reduction in sensitivities and better tracking performance in following desired reference power curves used in the simulations. Case scenarios are simulated demonstrating approximately 1.39dB transmit power savings compared to conventional methods.**

***Index Terms*—cognitive radio, energy efficiency, interference avoidance, quadratic approximator, transmission power control**

I. Introduction

Cognitive wireless communication systems, such as personal area networks [1], [2] can make use of the spectrum opportunistically for better utilization of licensed wireless bands. In this case, interference avoidance (IA) to licensed users is of paramount importance for continued co-existence. The unlicensed cognitive devices may also operate at the same frequencies, generating interference with each other. Transmit power control (TPC) algorithms are used to minimize both interference and energy consumption in these networks.

Considered networks might include various numbers of devices, new devices may connect the network during operations while some other devices may leave it, and connected wireless nodes may change their locations creating a dynamic time-varying and spatially variable coexistence environment. Receiver sensitivities may also be different and non-uniform. To address this diversity, adaptive and distributed TPC algorithms are typically used for the network self-organization [3]. Each wireless communication link is monitored by the receiver, which provides feedback to the linked transmitter for adaptive power adjustments. Predicting required power adjustments at each transmitter and their effects on overall network operation is a nontrivial task because of network diversity, complexity, and variability. Distributed network operation reduces traffic of overhead control data and shares computations among wireless nodes for faster self-organization and extended node life [4].

This paper addresses the power efficiency of adaptive TPC in terms of reduced total transmit power of the network by smoothing transmit power transients during adaptive iterations. It is achieved using a distributed closed loop power control system that applies to heuristically estimated dual-rate power adjustments during adaptive iterations. Bit error rate (BER) at the receiver serves as a quality of service (QoS) measure and is used directly to control transmit power. As maximum acceptable BERs are device specific, the algorithm is tailored to maintain required BERs.

State-of-the-art feedback approaches for power control already have been used. In [5], [6], and [7] signal-to-interference-plus-noise ratio (SINR) is estimated by the receiver and supplied to the transmitter for TPC operation. In [6] the authors eventually use SINR feedback for a joint strategy on power control and radio channel allocation, subject to constraints on transmission power and data traffic rates[8]. One feedback-based TPC algorithm is proposed in [9], called a distributed power controller (DPC), uses a well-known proportional integral derivative (PID) controller concept that produced a stable system and is used to adaptively tune PID gains. The controller input is the difference between actual

Corresponding author: Andre M. Mayers, andremayers@yahoo.com.

Andre M. Mayers, Patrick Benavidez, David Akopian, GVS Raju and Mo Jamshidi are with The University of Texas at San Antonio, Texas, San Antonio, 78249 (e-mail: pvc405@my.utsa.edu; gax646@my.utsa.edu; david.akopian@utsa.edu; gvs.raju@utsa.edu; jamshidi@utsa.edu).

received SINR and target SINR determined by QoS requirements.

However, according to the authors of [10], one problem with the SINR feedback-based methods is that they are constrained by the accuracy of SINR estimates in weak signal environments. In the proposed system, SINR feedback is replaced with BER estimates obtained from pilot subcarriers. Received pilot arrays are compared to expected arrays to estimate BERs. The receiver compares current BER with maximum allowed BER, makes a binary decision based on whether BER is acceptable or unacceptable and sends this decision to the transmitter. By so doing, the impact of errors associated with inaccurate BER measurement is mitigated. In addition, the proposed controller is different from conventional controllers because it is tailored to each device's long term response to channel conditions based on its specific maximum acceptable BER.

One should also note that the proposed system reduces the transmission power for an active established link. Other power-saving techniques in e.g. sensor networks [11] exploiting duty cycling by switching off the power [12], data reduction exploiting spatial or temporal correlation [13], optimization of routing paths [14], [15], resource allocation techniques trading off bandwidth for increased energy efficiency [8], etcetera can be integrated with the proposed method. The layout of the paper is as follows. Section II describes the system model and formulates the problem. Sections III and IV describe the algorithm and its analysis. Finally, Section V presents the results, which is followed by conclusions.

II. Simulation Test Bed and Problem Statement

The cognitive radio network may include a variety of devices as depicted in Fig. 1. The cognitive radio network includes so-called primary users (PU) and secondary users (SU). PUs are higher priority devices licensed by the network and SUs are the opportunistic devices exploiting underused channels. This paper addresses power control for SU devices.

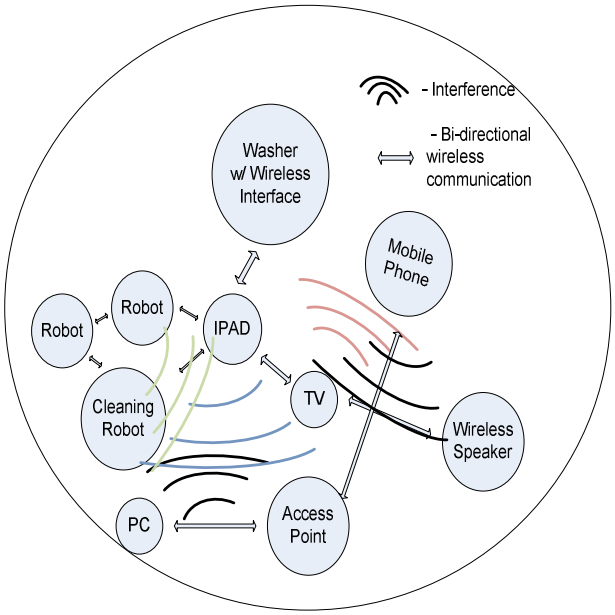

Fig. 1. System model.

Each pair of such devices is engaged in opportunistic, wireless, asymmetric bi-directional communication. Because of interoperability, devices can be members of multiple communication networks. The power control system operates separately for each communicating pair.

Cognitive radio (CR) technology allows devices to sense the spectrum, and adaptively bit load and allocate transmit power [10], [16], [17]. The devices use CR technology and a simulation test bed of this paper implements a WiMedia Alliance physical layer system, namely the multiband orthogonal frequency division multiplexing ultra-wideband (MB-OFDM UWB) system [18].

In state-of-the-art OFDM-based CR, often also called soft decision cognitive radio (SDCR) [19], both underused (underlay) and unused (overlay) spectral regions are exploited for more efficient communication [20]. Here, underlay refers to transmission in the presence of PU transmission (interference with SU), whereas overlay is transmission in the absence of PU transmission [21]. Symbols transmitted using underlay must overcome interference and additive white Gaussian noise (AWGN), whereas overlay must contend with only AWGN. This paper accepts the SDCR approach for applying the proposed power adaptation technique. In OFDM-based systems, BER feedback can be assessed using fixed subcarriers that are known as both transmitting and receiving devices. We refer to those as pilot subcarriers.

The system also follows environment specific restrictions imposed by the FCC concerning emitted power spectral density (PSD) [22]. For example, for indoors, a PSD of -41.3dBm/Mhz is allowed between 3.1-10.6 Ghz. Therefore, in the paper, S_{max} represents the total power allowed in a band.

We use the term channel users (CUs) to describe the presence of both primary and secondary user transmissions in the channel, which influence the transmission of the selected secondary user. We represent the PUs' transmission power using $P_i (i = 1, 2, 3, \ldots, \infty)$. The respective channel gains between the PUs and SU_T in subcarrier $j (j = 1, 2, 3, \ldots, 128)$ are represented by $h_{i,j}$, where i is the CU index. The problem statement follows.

A. Pre-adjusted Power Vectors $P_o(k)$, $P_u(k)$

Here we introduce the vectors $P_o(k)$, $P_u(k)$. In addition to S_{max}, we also cater for the possibility of limits on individual subcarriers within the MB-OFDM band. We refer to this limit as P_j^{sc}. Then, we can define the maximum possible transmit power for SU_T in a subcarrier j as

$$P_j^{SU_T} \triangleq P_j^{sc} - \left(n_o w + \sum_{i=1}^{M} h_{i,j} P_i \right) \quad (1)$$

where n_o is the AWGN PSD, and w is the bandwidth of a subcarrier, $n_o w + \sum_{i=1}^{M} h_{i,j} P_i$ is the power sensed in subcarrier j, and M represents the number of CUs.

Opportunistic or Secondary User (SU) transmit powers in a band are represented by $P_o(k)$ and $P_u(k)$. $P_o(k)$ is a vector of the SU unadjusted transmit powers in overlay subcarriers, which are subcarriers in which $\sum_{i=1}^{M} h_{i,j} P_i = 0$. The vector $P_u(k)$

comprises the SU unadjusted transmit powers in the underlay subcarriers, subcarriers in which $\sum_{i=1}^{M} h_{i,j} P_i > 0$. Because subcarrier powers are dynamically allocated based on time-varying subcarrier conditions at discrete time *k,*

$$[P_o(k), P_u(k)] = [P_{o,1}^{SU} \ldots P_{o,N_1(k)}^{SU}, P_{u,1}^{SU} \ldots P_{u,N_2(k)}^{SU}] \quad (2)$$

where $N_1(k)$ is the number of overlay subcarriers in a MB-OFDM band, and $N_2(k)$ is the number of underlay subcarriers.

B. Control Parameters $\lambda(k)$, $R_t(k)$, $e_o(k)$

At the receiver, $R_r(k)$ is the mean of the BER in the MB-OFDM pilot subcarriers. $R_r(k)$ is compared to $R_r^{\max}$, the maximum acceptable BER at the receiver (usually manufacturer defined) for a SU, and we obtain

$$\Delta R_r(k) = \begin{cases} 1, \text{ if } R_r(k) \le R_r^{\max} \\ -1, \text{ if } R_r(k) > R_r^{\max} \end{cases} \quad (3)$$

which is sent to the transmitter.

At the transmitter, parameter $R_t(k)$ is called the *memory-based feedback index* and is a function of BER feedback. At initialization $R_t(0) = \lambda_0 = \left(A \cdot R_r^{\max}\right)^{-1}$, where A is a scaling factor. $R_t(k)$ is iteratively updated using

$$R_t(k) = R_t(k-1) + \Delta R_r(k). \quad (4)$$

Also at the transmitter, a parameter $\lambda(k)$ is a dynamically adjusted benchmark that is a function of maximum acceptable BER. It is defined in an iterative manner as

initialize $\lambda(0) = \lambda_0$, $\lambda_C(0) = 0$

iterate time index k

$$\lambda_C(k) = \lambda_C(k-1) - \Delta R_r(k)$$

$$\lambda(\tau) = \begin{cases} \lambda(\tau-1) - 1, \ \lambda_C(k) = 0; \ \text{if } \lambda_C(k) > \lambda_T \\ \lambda(\tau-1) + 1, \ \lambda_C(k) = 0; \ \text{if } \lambda_C(k) < -\lambda_T \end{cases} \quad (5)$$

where λ_T is an integer threshold. In the BER feedback power control (BER-TPC) algorithm, the control error, $e_o(k)$ is defined by

$$e_o(k) = \lambda(k) - R_t(k) \quad (6)$$

The BER-TPC is effective using these two functions because $\lambda(k)$ is responsive to slow changing time-varying channel conditions and eventually stabilizes. The other function $R_t(k)$ is also memory-based, but is more responsive to the instantaneous changes in channel conditions (e.g. fast fade). The parameter $e_o(k)$, therefore, reflects the difference between the memory of the comparisons of BER feedback and maximum acceptable BER, and long-term performance. In addition, because the estimates of $R_t(k)$ are obtained from pilot subcarriers and the SU CR operates by selecting data-carrying subcarriers with good SINR, the BER for those subcarriers will be at least less than $R_t(k)$. The difference between BERs in pilot and data-carrying subcarriers degrades the performance of power control algorithms. The approach described above eliminates that particular problem by tracking performance using indices instead of using the difference at discrete time *k*.

C. Control Functions $\alpha_o(k)$, $\alpha_u(k) = f(R_t(k), \lambda(k), e_o(k), v)$

In this subsection, we introduce the control parameters for overlay and underlay symbols, $\alpha_o(k)$, $\alpha_\mu(k)$. First, $\alpha_o(k)$ is obtained using $e_o(k)$, which is tuned by normalizing using the dynamically adjusted benchmark, $\lambda(k)$. However, in light of consideration of the theoretically approachable time vs. power curve, we can cite Taylor's theorem, which states that if a function f is differentiable at point *a,* then it has a linear approximation at that point.

Let f be the function that produces the theoretical curve with $\alpha_o(k)$ necessary to result in BER $\simeq R_r^{\max}$. There exists a function g_n (the remainder of the Taylor series) such that the error in the quadratic approximation is

$$R_n(k) = f(k) - \alpha_{o_n} = g_n(k)(k-a)^2. \quad (7)$$

Given the limiting behavior of g_n, (7) approaches zero more quickly as n goes to infinity.

Therefore, to ensure faster convergence of the estimated power needed with actual power needed, we normalize $e_o(k)$ using $\lambda(k)^2$, which results in the quadratic tuner

$$\alpha_o(k) = 1 + \frac{e_o(k)}{\lambda(k)^2} = 1 + \frac{\lambda(k) - R_t(k)}{\lambda(k)^2} = 1 + \frac{1}{\lambda(k)} - \frac{R_t(k)}{\lambda(k)^2}. \quad (8)$$

We present further justification for the quadratic approximation in Section III. The underlay control parameter is obtained using

$$\alpha_u(k) = v^* \alpha_o(k) \quad (9)$$

where v is used to scale $\alpha_o(k)$. If $R_r(k) \ge R_r^{\max}$, underlay power is raised more quickly than overlay ($\alpha_u(k) = v^* \alpha_o(k)$) to overcome user interference. When $R_r(k) < R_r^{\max}$, underlay power is decreased less quickly than overlay $\left(\alpha_u(k) = \alpha_o(k) \big/ v\right)$.

D. Power control, BER-TPC and Comparative PID Algorithms

In the proposed system, transmit power is therefore adjusted using

$$P_T^{SU} = \vec{P}_o(k)^{\alpha_o(k)} + \vec{P}_u(k)^{\alpha_u(k)}, \quad (10)$$

where P_T^{SU} is the total power in a MB-OFDM band. The objective of the BER-TPC algorithm is to minimize P_T^{SU} through iterative adjustment of $\lambda(k)$, $R_t(k)$, while satisfying the constraints

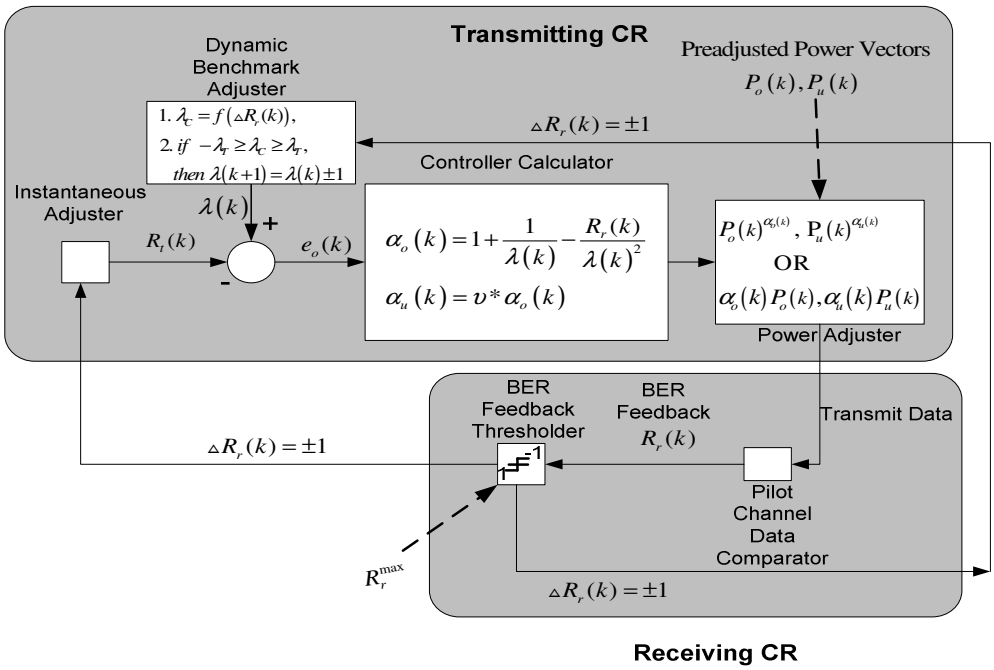

Fig. 2. BER-TPC system model

$$\sum_{i=1}^{M}\sum_{j=1}^{128} h_{i,j}P_i + P_T^{SU} \leq S_{\max}$$
$$R_e^{SU} \leq R_r^{\max}, \tag{11}$$

where R_e^{SU} is the SUs mean BER over the life of the transmission.

The BER-TPC minimization is heuristic. For comparative performance evaluation, a conventional PID controller is used as a reference. The power update equation for the PID controller is given by

$$P(k) = \partial e(k) + \beta x(k) = \theta[e(k) - e(k-1)] \tag{12}$$

in which $p(k)$ is the power at time k in a subcarrier, ∂, β and θ are the control parameters.

$$e(k) = \left[1 - \frac{\gamma_{\min}}{\gamma_a(k-1)}\right] p(k-1), \tag{13}$$

is calculated as the $(k-1)$ power, by the normalized difference between the achieved SINR, γ_a, from the $k-1$ transmission and the device's target SINR, γ_{min}. Finally,

$$x(k) = x(k-1) + e(k) \tag{14}$$

E. Overview of BER-TPC

Fig. 2 shows a model of the BER-TPC system. At the receiver, BER feedback is calculated at the pilot channel data comparator and passed to the BER feedback thresholder where it is compared to the maximum acceptable BER. The result $R_r(k)$ is sent to the transmitting CR. There, using the dynamic benchmark adjustor and the instantaneous adjustor, $\gamma(k)$ and $R_t(k)$ are updated. The error $e_o(k)$ is calculated and sent to the controller calculator, which results in an updated $\alpha_o(k)$. The latter, along with the input of the pre-adjusted power vectors $P_o(k)$, $P_u(k)$, is used to obtain the new power update.

III. JUSTIFICATION FOR SECOND ORDER APPROXIMATION IN CALCULATION OF $\alpha_o(k)$

We further justify using the second order approximation in the calculation of $\alpha_o(k)$ as follows. We introduce $R_{t,min}$ as the minimum acceptable value for $R_t(k)$. We also introduce $d_{max,Rt(k),\lambda(k)}$, which we define as the maximum possible deviation between $R_t(k)$ and $\lambda(k)$. Let us define a dynamic range for $R_t(k)$ and place further restrictions on $R_t(k)$, $R_{t,min}$:

$$R_t(k) \in [\lambda(k) - d_{max,R_t(k),\lambda(k)}, \lambda(k) + d_{max,R_t(k),\lambda(k)}] \tag{15}$$

$$R_{t,min} = -d_{max,R_t(k),\lambda(k)} \tag{16}$$

$$R_t(k) \in (R_{t,min}, \infty] \tag{17}$$

Because the lower bound for $\lambda(k)$ is 0, we can obtain a lower bound for (15) and (16). Desired operational behavior of error exponent approximation is obtained provided by the design rules and assumptions (i-iv), which provide bounded inputs and outputs:

i. Restriction in (15) provides acceptable oscillation magnitude in calculation of $\alpha_o(k)$ due to low sensitivity to $R_t(k)$.
ii. Assumption: Equation (15) and (16) are always true due to channel diversity and optimal channel switching in OFDM. As BER on one channel

decreases, another channel may be switched too, depending on BER and other criteria.

iii. Assumption: Given that $\lambda(k)$ tracks $R_t(k)$ by the dynamic range restrictions in (15), $\alpha_o(k) \approx 1$ as subject to the statement in (i). As $R_t(k)$ is approximately equal to the value of $\lambda(k)$ with maximum deviation $\pm d_{max,R_t(k),\lambda(k)}$, the value $\alpha_o(k)$ is always approximately equal to 1.

iv. Communication transceivers actual capabilities are limited by the receiver sensitivity and transmitter power; therefore, maximum and minimum values of $\alpha_o(k)$, $\lambda(k)$ and $R_t(k)$ are already set by physical conditions and limits of the transceiver.

We introduce the *ideal conditions* of the approximator, $\alpha_o(k) = 1$, where the power output is equal to the required power output based on the BER feedback $R_t(k)$, and where, with (15) and (16), criteria to meet the ideal condition is $\lambda(k) = R_t(k) \neq 0$. Let us also define 1st and 3rd order approximations for $\alpha_o(k)$ in (18) and (19) respectively, for use in comparison with the 2nd order approximation:

$$\alpha_o(k)_1 = 1 + \frac{\lambda(k) - R_t(k)}{\lambda(k)} = 2 - \frac{R_t(k)}{\lambda(k)} \qquad (18)$$

$$\alpha_o(k)_3 = 1 + \frac{\lambda(k) - R_t(k)}{\lambda^3(k)} = 1 + \frac{1}{\lambda^2(k)} - \frac{R_t(k)}{\lambda^3(k)} \qquad (19)$$

Furthermore, behavior of the approximator's operation near critical points at poles of $\alpha_o(k)$ function is described by the following:

$R_t(k) \approx R_{t,min}$:

i. $\Delta\alpha_o(k)$ is large in the 1st order approximator due to the $1/\lambda(k)$ term.

ii. $\Delta\alpha_o(k)$ in second and third order, approximators are reduced greatly as compared to 1st order approximator.

$R_t(k) \gg R_{t,min}$:

iii. $\Delta\alpha_o(k)$ is larger for the 1st order approximator than the 2nd and 3rd order approximators, but smaller in scale than that in case (i).

iv. $\Delta\alpha_o(k)$ is small for 2nd and 3rd order approximators.

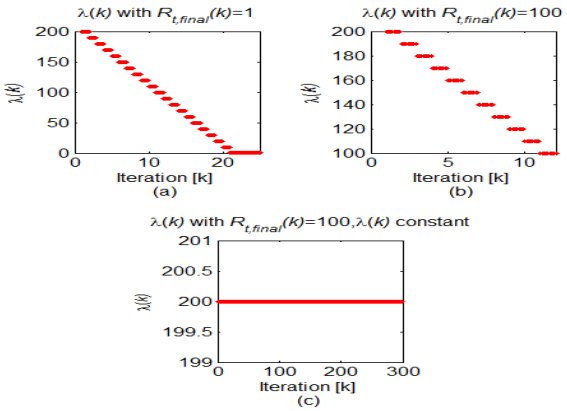

Fig. 3. Approximator inputs to test critical points of $\lambda(k)$: (a) tracking $R_t(k)$ as it decrements from a value of 200 to 1, (b) tracking $R_t(k)$ from 200 to 100, (c) not tracking $R_t(k)$ $\lambda(k)$ is constant.

In Fig. 3, $R_{t,final}(k)$ refers to the desired value of $R_t(k)$ that would result in the ideal approximator value. We evaluate the approximator performance with conditions given in (15), (16) and (17) for 1st, 2nd and 3rd order versions of error exponent approximations for $\alpha_o(k)$ (equations (18), (8), and (19), respectively), in Fig. 3. In the figure, a goal was set for the approximator to test the ideal criterion under critical values of $\lambda(k)$ in (8). Fig. 3a shows $\lambda(k)$ as it tracks $R_t(k)$a towards the critical value of 0 from $\lambda(k) = 200$, stopping at a near-critical value of 1. Fig. 3b shows when $\lambda(k)$ tracks a constant-valued $R_t(k)$ of 100 from an initial $\lambda(0)$ of 200. Fig. 3c shows the case where $\lambda(k)$ remains constant while $R_t(k)$ decreases from 200 to 1. Fig. 4 shows the profile and enhanced detail of $\alpha_o(k)$ for 1st, 2nd and 3rd order approximators for the input in Fig. 3.

We present the following conclusions on approximator performance based on the order of approximation. The first order approximator has a larger overshoot tracking the "ideal" line with $\alpha_o(k)$ underdamped. The second order approximator has significantly reduced overshoot, $\alpha_o(k)$ is damped, and tracks the "ideal" line well with fast convergence. Third order tracks the "ideal" line with minimal overshoot with $\alpha_o(k)$ overdamped. Given the results stated above, we decided that the second order approximation has ideal performance for our system.

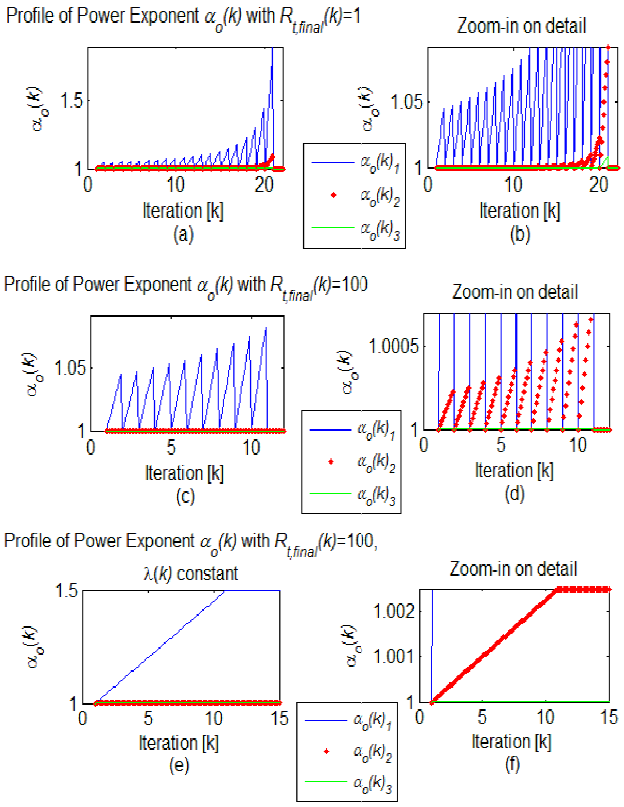

Fig. 4. Error exponent $\alpha_o(k)$ performance (a) for $R_{t,final} = 1$ for all values of t; (b) is enhanced detail of (a) for 2nd and 3rd order approximations, (c) is performance for $R_{t,final} = 100$ for all values of t; (d) is enhanced detail of (c) for 2nd order approximator; (e) is performance for $R_{t,final} = 200$ for all values of 'k' with $\lambda(k)$ constant value of 200; (f) is enhanced detail of (e) for the 3rd order approximator.

IV. Analysis of Relationships Between $\lambda(k)$, $\alpha_o(k)$, $e_o(k)$, and Transmit Signal Power.

In this section, we discuss the relationships between the control parameters, the stability, and operational range of $\alpha_o(k)$ in terms $\lambda(k)$.

A. *Stability of $\alpha_o(k)$ in terms of $\lambda(k)$*

Because power is adjusted by applying $\alpha_o(k)$ as an exponent to some real valued power, stability can be determined by examination of $\alpha_o(k)$. Rewriting $\alpha_o(k)$ in the form of the characteristic equation, we get $\lambda(k)^2 + \lambda(k) - R_t(k) = 0$. The zeros are at

$$\lambda_1(k), \lambda_2(k) = \frac{-1 \pm \sqrt{1 + 4*(R_t(k))}}{2}, \qquad (20)$$

where $\lambda_1(k)$ corresponds to the case in which the plus is used, and $\lambda_2(k)$ to case in which the minus is used. By observation of (8) the pole is at $\lambda(k) = 0$.

Therefore, stability is assumed if we bound the input such that we avoid the critical values $\lambda(k) \neq 0$, $\lambda_1(k)$, $\lambda_2(k)$.

B. *Operational range of $\alpha_o(k)$ in terms of $\lambda(k)$*

We determine the operational range of $\alpha_o(k)$ by observing the conditions over which $\alpha_o(k)$ is monotonic. We examine the behavior of $\alpha_o(k)$ using differentiation. Because control parameter $\alpha_o(k)$ has as inputs the unbounded $R_t(k)$ and $\lambda(k)$, it is necessary to partially differentiate $\alpha_o(k)$ in terms of $\lambda(k)$.

If we let $f(R_t(k), \lambda(k)) = 1 + \frac{1}{\lambda(k)} - \frac{R(k)}{\lambda(k)^2}$, then $\frac{\partial f(R_t(k), \lambda(k))}{\partial \lambda(k)} = \frac{2*R_t(k)}{\lambda(k)^3} - \frac{1}{\lambda(k)^2}$. The roots are at $\lambda(k)^{-2}$, and $\left(-1 + \frac{2*R_t(k)}{\lambda(k)}\right)$. Solving for $\lambda(k)$, we can define the operational range of $\alpha_o(k)$ in terms of $\lambda(k)$ with

$$0 < \lambda(k) < 2*R_t(k). \qquad (21)$$

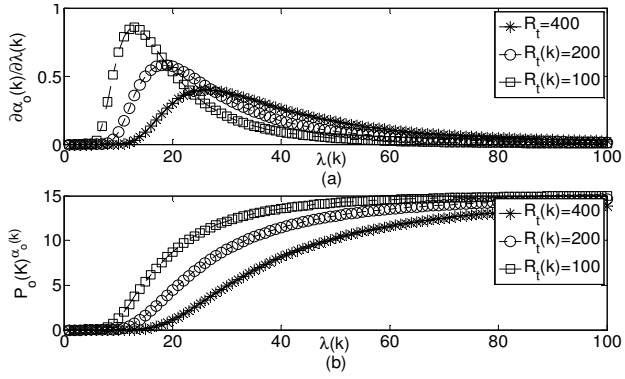

Fig. 5. For $R_t(k) = 400, 200, 100$ (a) $\lambda(k)$ vs. $\frac{\partial \alpha_o(k)}{\partial \lambda(k)}$ and (b) $\lambda(k)$ vs transmit signal power $[P_o(k)^{\alpha o(k)}]$.

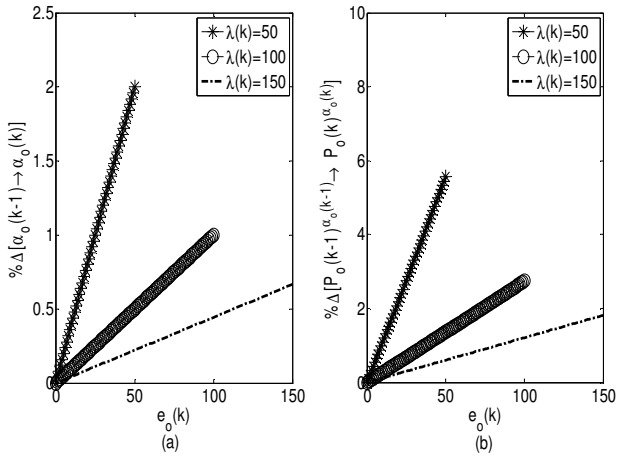

Fig. 6. For $\lambda(k) = (50, 100, 150)$ comparison of (a) the percentage of change in alpha from (k – 1) to (k) vs. the magnitude of $e_o(k)$ and (b) the percentage of change in transmit power from (k – 1) to (k) vs. the magnitude of $e_o(k)$.

V. Analysis Using Simulation

In this section we examine and discuss the relationships between transmit power and BER-TPC parameters. Fig. 5 and Fig. 6 are helpful in analyzing the relationships between transmit signal power, $\lambda(k)$ and $R_t(k)$. For example, let us assume the pre-adjusted power in the vector $P_o(k)$ is 15 dBW. Transmit signal power is obtained using the function $P_o(k)^{\alpha_o(k)}$. The parameter $\alpha_o(k)$ is obtained using (8). Fig. 5a shows $\partial \alpha_o(k) / \alpha \lambda(k)$, for $R_t(k)$ with instantaneous values of 400, 200, and 100. Fig. 5a shows that the rate of change is strongly influenced for values of $\lambda(k)$ close to zero. Fig. 5b demonstrates that transmit power grows more quickly when the magnitude of the error, $e_o(k)$, is greater. However, for comparable values of $\lambda(k)$, larger values of $R_t(k)$ result in slower growth.

For closer analysis on the effect of the magnitude of $e_o(k)$, we observe Fig. 5. In Fig. 6a, $e_o(k)$ is plotted against the percentage of change in a) $\alpha_o(k - 1)$ to $\alpha_o(k)$ and b) in transmit signal power for $\lambda(k) = (50, 100, 150)$. The relationships in both graphs are linear. For greater magnitudes of $e_o(k)$, the rate of change is greater. It is observable that for the same magnitudes of $e_o(k)$, smaller values of $\lambda(k)$ result in greater increases in transmit power. The power adjustment rate is calculable because (8)expressed in terms of the equation of a line, $y = mx + c$, gives

$$\alpha_o(k) = -\left(\frac{1}{\lambda(k)^2}\right) R_t(k) + \left(1 + \frac{1}{\lambda(k)}\right), \qquad (22)$$

where the rate, m, is $1 / \lambda(k)^2$.

A more general determination to be made from Fig. 5 and Fig. 6, is that the proposed system is indeed sensitive to device-specific QoS requirements. Because the benchmark $\lambda(k)$ is a scaled reciprocal of device maximum acceptable BER, devices with lower tolerances have higher-valued benchmarks. Observation of Fig. 6 shows that higher-valued benchmarks result in power adjustments of smaller magnitude. Thus, more sensitive devices are handled more carefully. In

addition, because the benchmarks are dynamic, the system has an internal mechanism for rate-adjustability of transmit power.

Fig. 7 shows the relationships between a) $\alpha_o(k)$ and transmit signal power and b) $\lambda(k)$ vs. $\alpha_o(k)$. $R_t(k)$ is held constant at 100. The relationship between $\alpha_o(k)$ and signal power is linear. In Fig. 7b, we observe that there is a logarithmic relationship between $\lambda(k)$ and $\alpha_o(k)$. There is a mirror effect for $\lambda(k) < 0$, which means that the reverse of the intended effect (increase/decrease in signal power) occurs after a zero crossing. Control parameter $\alpha_o(k)$ is also asymptotic for $\lambda(k) = 0$. Taking both observations into consideration clearly is why we stipulate $\lambda(k) > 0$.

More generally, Fig. 5b and Fig. 6b show that as long as $\lambda(k)$ is lower bounded at zero, the system is stable and predictable. Also, the logarithmic relationship demonstrates an asymptotic upper bound, which can be useful in establishing a de facto cap on maximum transmit power.

VI. Results and Simulations

The simulation parameters are as follows: modulation QPSK, line-of-sight (LOS) conditions, attenuation and path loss are assumed to be negligible, there are 14 bands with bandwidth of 528 Mhz. The bands are divided into 128 OFDM subcarriers with designated pilot, guard, and null subcarriers, data rate 10Mbit/s, transmitted data 10Mb, subcarrier interference (PU) power is generated using a continuous uniform distribution over a range of 0dBm to 30.3dBm, S_{max} 47 dBm to 49 dBm, and BER reference value over the range 10e-3 to 10e-6. Typical OFDM transmission is followed, except the TPC methods are applied after band and subcarrier selection, and before modulation and bit loading. In all simulations, BER is the BER in the data carrying subcarriers. Simulation was done for SU node densities of 0.0033, 0.01, 0.0167, and 0.03 *devices/m*^{3} randomly located on a three dimensional grid. Device coordinates were independently generated using a continuous uniform random distribution. Path loss (dB) between the i^{th} and j^{th} devices is given by

$$L_{i,j} = (d_{i,j})^{-\gamma} \tag{23}$$

where $d_{i,j}$ is distance between devices and $\gamma = 3.4$ is the path loss exponent.

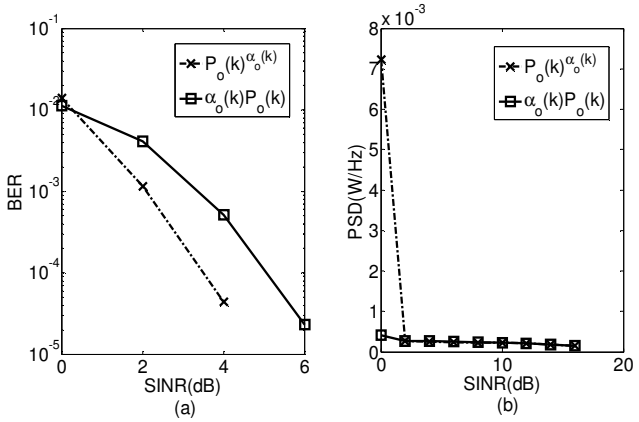

Fig. 7. Comparison of $\alpha_o(k)$ and $\alpha_u(k)$ used in BER-TPC as exponent and scalar for SINR vs. a) BER and b) PSD(W/Hz).

TABLE I.

	C(DPC)	*C(SNR)*	*1st Order*
BER (dB)	+5.65	+6.73	+8.16
PSD (dB)	+3.6	+1.39	+1.11

Comparison of PID, SNR and 1st order BER-TPC controllers to the 2nd order BER-TPC in terms of BER and transmit PSD (W/Hz) for SINR over the range [0:20] dB

TABLE II.

	$\upsilon = 1.5$	$\upsilon = 2$	$\upsilon = 2.5$
BER (dB)	-.01	-.18	+0.02
BER (%)	-.45%	-4%	+0.5%
PSD (dB)	+.005	+.05	-0.18
PSD (%)	+.12	+1.21	-4.1

Comparison of change in BER and PSD for underlay power adjusted at three difference rates, for SINR over the range [0:20]dB. The rates are compared to when underlay and overlay signal power is adapted at the same rate ($v = 1$).

From Fig. 7, we can compare a) BER and b) PSD (W/Hz) for $\alpha_o(k)$ and $\alpha_u(k)$ used in power control as either an exponents or a coefficient. On average, BER is approximately 1.9 dB less when overlay and underlay signal power are adjusted using $P_o(k)^{\alpha_o(k)}, P_u(k)^{\alpha_u(k)}$ as opposed to $\alpha_o(k)*P_o(k)$, $\alpha_u(k)*P_u(k)$. PSD is higher when the alphas are used as exponents at SINR equal to 0 dB, but for SINR > 1, PSD in both cases are similar. Therefore, for all other simulations we calculate transmit power using $\alpha_o(k)$ and $\alpha_u(k)$ as exponents $\left(P_o(k)^{\alpha_o(k)}, P_u(k)^{\alpha_u(k)}\right)$.

Table I shows the performance of the DPC, SNR and 1st order BER-TPC controllers in comparison to the 2nd order BER-TPC. The control parameters for the DPC controller (12), *C(DPC)*, are $\partial = 0$, $\beta = -1$, $\theta = 1$. The controller *C(SNR)* represents Hoven and Sahai's [7] SNR-constrained controller. In the *C*(*SNR*) the transmitter adjusts transmit power based on the assessment of noise/interference at the receiver, and the need to meet a predefined SNR. The SNR estimation is generated from a random Gaussian distribution with mean = actual interference, and variance = 0.5dB. Under the S_{max} constraint, in terms of BER, the 2nd order BER-TPC outperforms the DPC controller with 5.65 dB lower BER, the SNR controller with 6.73 dB lower BER, and with 8.16 dB lower BER than the 1st order controller (18). In terms of transmit power, the SNR controller uses 1.2 dB more than the 2nd order BER-TPC controller. The 2nd order BER-TPC controller also outperforms the DPC and the 1st order BER-TPC controllers, which respectively use 3.6 dB and 1.11dB more transmit power. It is evident that under constraints on radiated power for SUs, the BER-TPC exhibits superior overall performance in terms of reducing transmit power while maintaining QoS in terms of restricting BER.

Table II shows BER and PSD (W/Hz) (compared in terms of dB and percentages) for the power control algorithm with underlay signal power (*underlay_power=overlay_ power**/ ÷ *v*) adjusted at different ratios ($v = 1.5, 2, 2.5$) to overlay power. The change in dB and percentage for $v = 1.5, 2, 2.5$ are compared to the case $v = 1$. We know that $e_o(k)$ determines the size of the increments of power adjustment for overlay signals. The parameter $\alpha_o(k)$ is calculated using $e_o(k)$, while $\alpha_u(k)$ is

calculated using $e_o(k)$ and v (see (9)). If $R_r(k) > R_e^{\max}$ underlay power is increased more quickly than overlay power ($e_u(k) = e_o(k)*v$). When $R_r(k) \le R_e^{\max}$ underlay power is decreased less quickly than overlay ($e_u(k) = e_o(k)/v$). In the best scenario, when $v = 2$, the BER for $0 \le SINR(dB) \le 20$ is 4% lower than $v = 1$. PSD is increased by 1.21%, however. The $v = 2.5$ returns the best savings in PSD at 4.1% but with a 0.5% increase in BER

The results in Table II are relevant in an environment in which opportunistic users are using both underlay and overlay techniques. It is clear that the value of v can be manipulated to obtain tradeoffs in either reducing BER and or reducing transmit power. For overall transmit power savings, we can set $v = 2.5$, to reduce BER set $v = 2$.

VII. Conclusion

In this paper, we proposed a novel distributed energy saving adaptive transmit power control system for SU CRs. The proposed system allows SUs to approximate the minimum transmit power needed while maintaining (QoS), practicing IA to primary users, and observing spectral power emission limits. We established operational bounds for stability upon the control system, and showed that under restrictions on radiated power, power savings of at least 1.39 dB can be realized in comparison to the conventional SNR feedback controllers. It was also shown that the 2nd order BER-TPC approximator outperforms a 1st order BER-TPC approximator in terms of restricting transmit power and BER. We also demonstrated that underlay signal power could be adjusted at a different ratio to overlay signal power to either conserve power or lower BER.

VIII. References

[1] T. Zahariadis, "Personal Area Networks," *Commun. Eng.*, vol. 1, no. 3, pp. 12–15, Jun. 2003.

[2] M. Chen, S. Gonzalez, A. Vasilakos, H. Cao, and V. C. M. Leung, "Body Area Networks: A Survey," *Mob. Netw. Appl.*, vol. 16, no. 2, pp. 171–193, Aug. 2010.

[3] E. Dall'Anese, S.-J. Kim, G. B. Giannakis, and S. Pupolin, "Power Control for Cognitive Radio Networks Under Channel Uncertainty," *IEEE Trans. Wirel. Commun.*, vol. 10, no. 10, pp. 3541–3551, Oct. 2011.

[4] M. I. Razzak, B. A. Elmogy, M. K. Khan, and K. Alghathbar, "Efficient distributed face recognition in wireless sensor network," *Int. J. Innov. Comput. Inf. Control*, vol. 8, no. 4, pp. 2811–2822, 2012.

[5] E. C. Peh, Y.-C. Liang, and Y. Zeng, "Sensing and power control in cognitive radio with location information," in *Communication Systems (ICCS), 2012 IEEE International Conference on*, 2012, pp. 255–259.

[6] M. Yu, X. Ma, W. Su, and L. Tung, "A new joint strategy of radio channel allocation and power control for wireless mesh networks," *Comput. Commun.*, vol. 35, no. 2, pp. 196–206, Jan. 2012.

[7] N. Hoven and A. Sahai, "Power scaling for cognitive radio," in *Wireless networks, communications and mobile computing, 2005 International Conference on*, 2005, vol. 1, pp. 250–255.

[8] S. Videv and H. Haas, "Energy-efficient scheduling and bandwidth-energy efficiency trade-off with low load," in *Communications (ICC), 2011 IEEE International Conference on*, 2011, pp. 1–5.

[9] A. Paul, M. Akar, M. G. Safonov, and U. Mitra, "Adaptive Power Control for Wireless Networks Using Multiple Controllers and Switching," *IEEE Trans. Neural Netw.*, vol. 16, no. 5, pp. 1212–1218, Sep. 2005.

[10] R. Tandra and A. Sahai, "SNR Walls for Signal Detection," *IEEE J. Sel. Top. Signal Process.*, vol. 2, no. 1, pp. 4–17, Feb. 2008.

[11] G. Anastasi, M. Conti, M. Di Francesco, and A. Passarella, "Energy conservation in wireless sensor networks: A survey," *Ad Hoc Netw.*, vol. 7, no. 3, pp. 537–568, 2009.

[12] S. Jin, W. Yue, and Q. Sun, "Performance analysis of the sleep/wakeup protocol in a wireless sensor network," *Int. J. Innov. Comput. Inf. Control*, vol. 8, no. 5, pp. 3833–3844, 2012.

[13] M. C. Vuran, Ö. B. Akan, and I. F. Akyildiz, "Spatio-temporal correlation: theory and applications for wireless sensor networks," *Comput. Netw.*, vol. 45, no. 3, pp. 245–259, Jun. 2004.

[14] C. Han, T. Harrold, S. Armour, I. Krikidis, S. Videv, P. M. Grant, H. Haas, J. S. Thompson, I. Ku, and C.-X. Wang, "Green radio: radio techniques to enable energy-efficient wireless networks," *Commun. Mag. IEEE*, vol. 49, no. 6, pp. 46–54, 2011.

[15] A. Papadopoulos, A. Navarra, J. A. McCann, and C. M. Pinotti, "VIBE: An energy efficient routing protocol for dense and mobile sensor networks," *J. Netw. Comput. Appl.*, vol. 35, no. 4, pp. 1177–1190, Jul. 2012.

[16] J. Miroll and T. Herfet, "Efficient OFDM-based WLAN-multicast with feedback aggregation, power control and rate adaptation," *Comput. Commun.*, vol. 35, no. 18, pp. 2245–2253, Nov. 2012.

[17] N. Devroye, M. Vu, and V. Tarokh, "Cognitive radio networks," *IEEE Signal Process. Mag.*, vol. 25, no. 6, pp. 12–23, Nov. 2008.

[18] D. Cabric and R. W. Brodersen, "Physical Layer Design Issues Unique to Cognitive Radio Systems," in *IEEE 16th International Symposium on Personal, Indoor and Mobile Radio Communications*, Berlin, 2005, vol. 2.

[19] Z. Wu and B. Natarajan, "Interferent tolerant agile cognitive radio: Maximize channel capacity of cognitive radio," presented at the 4th IEEE Consumer Communications and Networking Conference, 2007, pp. 1027–1031.

[20] V. D. Chakravarthy, Z. Wu, A. Shaw, M. A. Temple, R. Kannan, and F. Garber, "A general overlay/underlay analytic expression representing cognitive radio waveform," in *Waveform Diversity and Design Conference, 2007. International*, 2007, pp. 69–73.

[21] R. Menon, R. M. Buehrer, and J. H. Reed, "Outage Probability Based Comparison of Underlay and Overlay Spectrum Sharing Techniques," *New Front. Dyn. Spectr. Access Neworks*, pp. 101–109, 2005.

[22] Federal Communications Commission, "FCC notice of proposed rule making, revision of part 15 of the commission's rules regarding ultra-wideband transmission systems." ET-Docket 98-153.